



Cite this: DOI: 10.1039/d6sc02543a

All publication charges for this article have been paid for by the Royal Society of Chemistry

Formation of the intradimer disulfide bond in human calprotectin maintains metal-withholding function and tunes proteolytic susceptibility

Aurelio Mollo,^a Emma Y. Cool,^a Bahar Sakar,^a Kushol Gupta^b and Elizabeth M. Nolan^{*a}

Human calprotectin (CP, S100A8/S100A9 oligomer, MRP8/MRP14 oligomer) is a metal-sequestering protein that contributes to nutritional immunity. Each human CP subunit contains a single Cys residue—Cys42 in S100A8 and Cys3 in S100A9—and recent reports have revealed that these residues can undergo disulfide bond formation resulting in a covalently linked heterodimer species, hereafter referred to as disulfide-linked CP (dslCP). Nevertheless, the biochemical and functional consequences of this intradimer disulfide linkage are largely unknown. Here, we report a robust reconstitution and purification protocol affording dslCP and present initial biochemical and functional evaluation of the protein. Our investigations demonstrate that dslCP undergoes Ca(II)-dependent self-association to form heterotetramers, depletes multiple metals from bacterial growth media, and induces an iron-starvation response in diverse bacterial pathogens. The intradimer disulfide linkage exhibits a midpoint potential of -213 mV, indicating that it can become oxidized in the extracellular space. Studies of enzymatic disulfide bond reduction reveal that divalent cation binding renders dslCP a poor substrate for the thioredoxin system. Investigations of proteolytic stability show that the intradimer disulfide linkage in dslCP enhances the susceptibility of the protein scaffold to digestion by human neutrophil elastase and trypsin, supporting a model wherein oxidative post-translational modifications direct protein lifetime. Our work expands upon the known roles of post-translational modifications of CP and highlights the need for further studies to define how oxidative modifications regulate the structure, stability, and function of this important host-defense protein.

Received 27th March 2026
Accepted 3rd June 2026

DOI: 10.1039/d6sc02543a

rsc.li/chemical-science

Introduction

During the human innate immune response, neutrophils deploy numerous immune factors to defend the host, including antimicrobial peptides, proteases, metal-sequestering proteins, and reactive oxygen species.^{1,2} Calprotectin (CP), a hetero-oligomer of S100A8 (MRP8, calgranulin A, α subunit) and S100A9 (MRP14, calgranulin B, β subunit), is an abundant host-defense protein produced and released by neutrophils that participates in nutritional immunity by sequestering nutrient metal ions in the extracellular space.^{3–6} Numerous studies to date have addressed the molecular basis for metal sequestration by CP, and these efforts have largely focused on two oligomeric forms of CP: the $\alpha\beta$ heterodimer and the $(\alpha\beta)_2$ heterotetramer.^{6–11} Nevertheless, biochemical investigations of CP and clinical studies that detected CP subunits in patient samples indicate that CP speciation is much more complex. In

addition to the $\alpha\beta$ and $(\alpha\beta)_2$ oligomeric states and multiple possible metal-bound forms, compelling evidence for various post-translationally modified CP species exists.^{12–24} Advancing our understanding of how CP functions at the host–pathogen interface requires consideration of these additional forms. In this work, we investigate a recently recognized oxidative post-translational modification (PTM) of human CP—an intradimer disulfide linkage between Cys42 of S100A8 and Cys3 of S100A9—and its implications for the structure and function of the protein.

The S100A8 and S100A9 subunits each contain two EF-hand domains for Ca(II) binding, and apo CP exists as the $\alpha\beta$ heterodimer.^{8,9} When the EF-hands coordinate Ca(II) ions, a conformational change occurs, including the repositioning of hydrophobic residues that compose the tetramer interface and the self-association of two heterodimers.^{10,11,25,26} Formation of the Ca(II)-bound $(\alpha\beta)_2$ heterotetramer leads to increased proteolytic stability²⁷ and enhanced binding affinities for divalent transition-metal ions.^{28–31} CP has two transition-metal binding sites that coordinate Mn(II),^{29,32,33} Fe(II),³⁰ Co(II),²⁸ Ni(II),³¹ Cu(I/II),³⁴ and Zn(II).^{28,33,35} These sites form at the S100A8/S100A9 interface and contain metal-coordinating residues from

^aDepartment of Chemistry, Massachusetts Institute of Technology, Cambridge, MA 02139, USA. E-mail: lnolan@mit.edu; Tel: +1-617-452-2495

^bDepartment of Biochemistry & Biophysics, Perelman School of Medicine, University of Pennsylvania, Philadelphia, PA 19104, USA



each subunit (Fig. 1A). Site 1 is a His₃Asp motif that coordinates Zn(II) and Cu(I/II) with high affinity,^{28,34,35} whereas site 2 is a His₆ motif that complexes Mn(II), Fe(II), Ni(II), Cu(I/II) and Zn(II) with high affinity.^{6,29–32,34–36} This high-affinity binding allows CP to sequester multiple metal nutrients in the extracellular space and thereby contribute to nutritional immunity.

The current working model for CP in nutritional immunity is based on its biological coordination chemistry and observations from many host–pathogen studies.⁶ In this model, CP exists as an αβ heterodimer in the low Ca(II) environment of the neutrophil cytoplasm. Following release into the extracellular space where Ca(II) levels are high (~2 mM),³⁷ CP binds Ca(II) ions and undergoes self-association to form the (αβ)₂ heterotetramer, which is the metal-sequestering form that competes with microbial pathogens for available divalent transition-metal ions. Indeed, the sequestration of metal nutrients by CP induces metal starvation responses in bacterial and fungal pathogens, supporting its role in nutritional immunity.^{5,31,34,38–41} This working model is centered on studies of the heterodimeric and tetrameric forms of CP in the absence of PTMs, which may have as-yet undetermined structural and functional consequences. Thus, an important next step is to integrate an understanding of how various PTMs may affect CP structure as well as its self-association properties, metal-binding abilities, and other functional characteristics.

To date, post-translationally oxidized S100A8 and S100A9 species have been detected in various patient samples and murine specimens.^{12–23} Mass spectrometric analyses have identified CP subunits containing methionine sulfoxide (MetO) in various human samples, including sputum, kidney stones, nasal mucus, and pimple pus.^{12,14–16,18,19,21} Cysteine oxidations have also been reported for S100A8 and S100A9 in studies of human samples, including *S*-nitrosylation, *S*-glutathionylation, and *S*-cysteinylation, as well as oxathiazolidine dioxide, sulfinic acid, sulfonic acid, and disulfide bond formation.^{12,14,15,20,21} Notably, human CP has only two Cys residues, one in each

subunit (Table S1). Cys42 of S100A8 is adjacent to the hinge region, a flexible linker between the N- and C-terminal EF-hands, and Cys3 of S100A9 is in the disordered N-terminal region (Fig. 1B). An early study of the CP heterodimer concluded that S100A8(C42) and S100A9(C3) are not proximal enough to form a biologically relevant intradimer disulfide bond based on homology modeling using the solution-state structure of S100A6.⁹ Subsequently, many investigations employed the Cys-null CP-Ser variant [S100A8(C42S)/S100A9(C3S)],^{9,28,30,34,40} and comparative studies employing both CP and CP-Ser have largely supported the notion that the Cys → Ser substitution has negligible structural and functional consequences.^{28,30,40} Nevertheless, evidence for disulfide bond formation between Cys42 and Cys3 of the S100A8 and S100A9 subunits of CP was found during mass spectrometry studies of human saliva and bronchoalveolar lavage fluid.^{15,20} These observations suggested a potential aspect of CP structure that has been largely overlooked and may have relevance to the function and fate of CP at infection and inflammation sites. Moreover, two recent biochemical studies uncovered an oxidized CP species with the intradimer Cys42–Cys3 disulfide bond, hereafter named dslCP (disulfide-linked CP), in samples that were subjected to chemical oxidation or the neutrophil oxidative burst.^{19,20} Both investigations concluded that formation of this disulfide bond increased the proteolytic susceptibility of the CP protein scaffold, affording a model in which this PTM modulates protein lifetime. One limitation of this prior work was that both studies examined unpurified oxidation reaction mixtures.^{19,20} These intriguing observations indicate that a detailed biochemical and functional evaluation of a dslCP isolate is warranted to further understand the consequences of the presence of the intradimer disulfide bond for protein structure as well as biological function and fate.

In the present work, we report a robust method for the reconstitution and purification of dslCP and probe various biochemical and functional consequences of intradimer disulfide bond

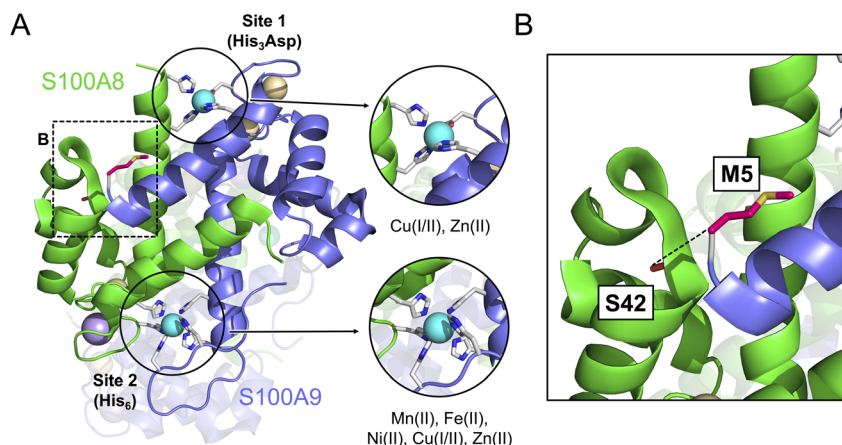


Fig. 1 Structural features of CP. (A) Crystal structure of the Ni(II)-, Ca(II)- and Na(I)-bound CP-Ser heterotetramer. The dashed box indicates the region expanded in (B), a close-up view indicating the proximity between S100A8(S42) and S100A9(M5). The N-terminal tail of S100A9 is disordered, so Met1 through Lys4 are not observed; the approximate location of the disulfide bond is indicated with a dashed line. One of the two heterodimers is presented as transparent. Ni(II), Ca(II) and Na(I) ions are shown as cyan, yellow, and purple-colored spheres, respectively. The locations and metal-binding preferences of the two metal-binding sites are indicated (circular insets), with the side chains of the residues involved shown in grey. The oxidation state(s) of sequestered Cu is unclear and is thus denoted as Cu(I/II). PDB ID 5W1F (ref. 31).



formation in CP. We demonstrate that dslCP forms Ca(II)-bound heterotetramers, depletes transition metals from microbial growth media, exhibits antimicrobial activity, and induces iron starvation responses in bacterial pathogens. We also show that Ca(II)-induced tetramerization is perturbed and establish that formation of the intradimer disulfide bond enhances the proteolytic susceptibility of CP, which is likely a consequence of conformational changes to the protein scaffold. These results provide further evidence that oxidative PTMs modulate the biological fate of CP and allow us to further integrate dslCP into the working model for CP in nutritional immunity.

Results

Preparation of dslCP

We sought to obtain dslCP, the disulfide-linked heterodimer, in sufficient purity and quantity for further study using the purified CP heterodimer containing two free Cys residues as the starting material. We aimed to identify conditions that would afford (i) near-quantitative conversion of CP to dslCP in a reasonable timeframe; (ii) negligible side reactions that would reduce yield and complicate purification; and (iii) a straightforward purification to isolate dslCP. Prior investigations of other S100 proteins that can harbor disulfide bonds, including human S100A7,⁴² murine S100A8,⁴³ and bovine S100B,⁴⁴ utilized Cu(II)-mediated oxidation to access the respective disulfide-containing species. However, the observed tendency of CP to precipitate in the presence of excess Cu(II) and the anticipated need to remove bound and/or contaminating Cu led us to favor other oxidants. We considered performing disulfide-bond exchange reactions between the CP heterodimer and oxidized glutathione (GSSG) or oxidized DTT (DTT_{ox}), but preliminary reaction screening indicated only slow conversion of CP to dslCP in the presence of excess GSSG (Fig. S1A), and negligible dslCP formation in the presence of excess DTT_{ox} (Fig. S1B). Thus, we turned our attention to using hydrogen peroxide (H₂O₂) as an oxidant. In our prior work examining post-translational Met and Cys oxidation,¹⁹ we used relatively low concentrations of H₂O₂ (100 μM) that favored disulfide-bond formation over Met oxidation to generate disulfide-linked forms of CP—including dslCP and the S100A9–S100A9 linked heterotetramer—on an analytical scale. In this prior work, we observed that the S100A9–S100A9 heterotetramer converted to dslCP over time, indicating that the S100A8–S100A9 intradimer disulfide linkage is thermodynamically favored. Thus, we investigated the feasibility of implementing this approach on a preparative scale to obtain dslCP without the formation of confounding Met-oxidized species.

We first tested the analytical-scale reaction conditions on a preparative scale by incubating 20 mg of CP with 100 μM H₂O₂ at pH 8.0 over a 24 h period and monitoring the reaction by analytical HPLC. These conditions resulted in high conversion rates for disulfide bond formation and generation of dslCP (>90%), but evidence for Met oxidation was observed in the HPLC traces (Fig. S2, Table S5). We then tested lower H₂O₂ concentrations and found that 20–35 μM H₂O₂ afforded a similar conversion rate to dslCP while minimizing unwanted

Met oxidation (Fig. S3). Moreover, varying the buffer pH over the 7.0–9.5 range had a negligible effect on dslCP formation (Fig. S4). Further analysis of the reaction mixtures by Western blot showed that dslCP was the major product but that the mixtures contained some unreacted CP (indicated by S100A8_{red} and S100A9_{red}), as well as species with disulfide linkages between S100A8–S100A8 and S100A9–S100A9 (hereafter referred to as S100A8_{ox} and S100A9_{ox}; Fig. 2A, Table S2). These latter species indicated the formation of interdimer disulfide bonds that afford disulfide-linked heterotetramers. The species were not further characterized; their identities were inferred based on a combination of apparent molecular weight, antibody reactivity, and our prior work.¹⁹ Consistent with previous reports,^{19,20} the S100A9–S100A9 species appeared to be a kinetically favored product that was produced early on (up to 6 h post-H₂O₂ addition) but was then consumed as the thermodynamically favored dslCP species accumulated (Fig. 2A). We isolated dslCP from this mixture by utilizing anion exchange chromatography, with buffers at pH 9.5 (Fig. 2B). We reasoned that basic pH would deprotonate the free cysteines in CP, affording a different formal charge for CP compared to dslCP and thereby facilitating separation of these two species. SDS-PAGE of the protein-containing fractions obtained from anion exchange chromatography indicated that the procedure afforded separation of dslCP from S100A8_{ox} and S100A9_{ox} and that trace CP, indicated by the S100A8_{red} and S100A9_{red} subunit bands, was present in most fractions (Fig. 2C, D and S5). Overall, this procedure was highly reproducible and typically afforded dslCP in 10–40% yield. To further support the assignment of dslCP as the disulfide-linked species containing the Cys42–Cys3 disulfide bond, we performed thiol quantification, which revealed no free thiols in dslCP (Table S6), as well as trypsin digest and mass spectrometry, which allowed us to unambiguously identify the Cys42–Cys3 linkage (Fig. S6–S8 and Table S7).

dslCP is α -helical and undergoes Ca(II)-dependent heterotetramerization

We examined the secondary structure and oligomerization properties of dslCP to obtain initial insights into the structural consequences of the disulfide linkage. The circular dichroism (CD) spectra of dslCP in the absence and presence of excess Ca(II) showed features characteristic of an α -helical structure and closely resembled the spectra of CP (Fig. S9).²⁸ This comparison indicated that the intradimer disulfide bond in dslCP has negligible impact on the overall secondary structure of the CP protein scaffold in both the absence and presence of Ca(II). Thermal denaturation of dslCP revealed that, as observed for CP, the thermal stability of dslCP increased upon Ca(II) addition (Fig. S10). CP exhibited T_m values of 73 °C in the absence of Ca(II) and 86 °C in the presence of Ca(II). These values were in good agreement with the T_m values previously reported for CP-Ser, which were 59 °C and 79 °C in the absence and presence of Ca(II), respectively (Table S8).²⁸ Similarly, the unfolding curve of dslCP in the presence of excess Ca(II) had a single transition at 85 °C. In the absence of Ca(II), most dslCP unfolding occurred at lower temperatures than observed for the



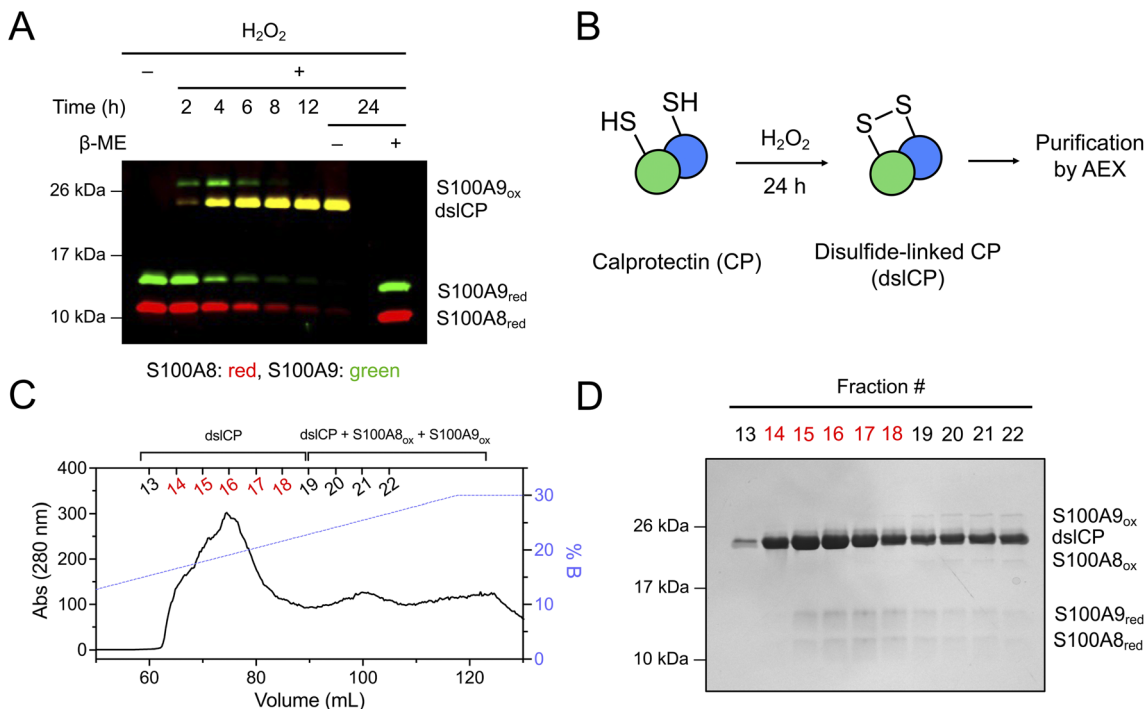


Fig. 2 Preparation of dslCP. (A) Time-course Western blot showing dslCP formation from the CP heterodimer and its reduction by β -mercaptoethanol (β -ME) to the constituent S100A8 and S100A9 subunits. S100A8 was stained red and S100A9 was stained green; yellow indicates overlapping signals. (B) Overview of the dslCP-forming reaction, involving incubation in H_2O_2 -supplemented buffer, followed by anion exchange chromatography (AEX). (C) Anion exchange chromatogram of a representative oxidation reaction after 24 h. The reaction mixture was adjusted to pH 9.5 and eluted at the same pH in a buffer consisting of 20 mM Tris and an NaCl gradient (0 \rightarrow 300 mM NaCl over 15 column volumes, 1 mL min^{-1}). Fraction numbers (13–22) are indicated above the chromatogram. The volume corresponds to volume post-injection. (D) SDS-PAGE analysis of the anion exchange chromatography fractions from panel C. For this purification, fractions 14–18 (highlighted red in panels C and D) were pooled to afford dslCP.

+Ca(II) samples; however, its unfolding profile showed variable behavior across samples, and some samples did not exhibit a clear singular unfolding transition (Fig. S11). Overall, these data indicate that dslCP also exhibited Ca(II)-dependent stabilization and that the unfolding of apo dslCP differed from that of CP for reasons that are currently unclear.

We employed analytical size exclusion chromatography (SEC) to ascertain whether dslCP undergoes Ca(II)-dependent self-association, a hallmark of the quaternary structure of CP (Fig. 3 and Table S9). In the absence of added Ca(II) in the protein sample and running buffer, dslCP eluted at 11.1 mL, which corresponded to a molecular weight of 36 kDa and is assigned to the 24 kDa disulfide-linked $\alpha\beta$ heterodimer (Fig. 3A). Upon the addition of excess Ca(II) to the sample and running buffer, dslCP eluted at 10.5 mL, which corresponded to a molecular weight of 47 kDa and indicates that dslCP undergoes Ca(II)-dependent formation of an $(\alpha\beta)_2$ heterotetramer. The analytical SEC profiles of dslCP are highly similar to those of CP, which eluted at 11.1 mL (36 kDa) and 10.4 mL (48 kDa) in the absence and presence of Ca(II), respectively. These results were in agreement with previously reported molecular weight values obtained from analytical SEC.²⁸ To further examine Ca(II)-dependent self-association by dslCP, we performed Ca(II) titrations in which increasing Ca(II) equivalents were added to the protein samples and Ca(II) was omitted from the running buffer. A comparison of

the resulting chromatograms for dslCP and CP indicated that dslCP requires higher Ca(II) equivalents to fully tetramerize (Fig. 3B). For instance, when the proteins were pre-incubated with 16 equiv of Ca(II), the chromatogram for the CP sample exhibited a single peak at 10.4 mL (48 kDa). In contrast, the chromatogram for dslCP also contained a peak at 10.4 mL, but a marked shoulder of higher elution volume was also present. This result indicated incomplete conversion of dslCP to the $(\alpha\beta)_2$ heterotetramer. This comparison suggested that the intradimer Cys42–Cys3 disulfide bond in dslCP somewhat perturbs Ca(II)-induced self-association relative to CP. Nonetheless, these data indicate that dslCP will form heterotetramers in the extracellular environment, where Ca(II) concentrations are ~ 2 mM (ref. 37) and in excess of reported concentrations of CP in human samples (up to 1000 $\mu\text{g mL}^{-1}$, or ~ 40 μM heterodimer).⁴⁵ These results also allowed us to conceptualize dslCP as a heterotetramer species in our subsequent experiments designed to probe the functional properties of the protein, which were conducted under high Ca(II) conditions to mimic the extracellular space.

dslCP depletes multiple nutrient metals from microbial growth media

To obtain preliminary insight into whether the intradimer disulfide bond might affect the metal sequestration properties of dslCP, we performed metal-depletion studies using dslCP, CP,



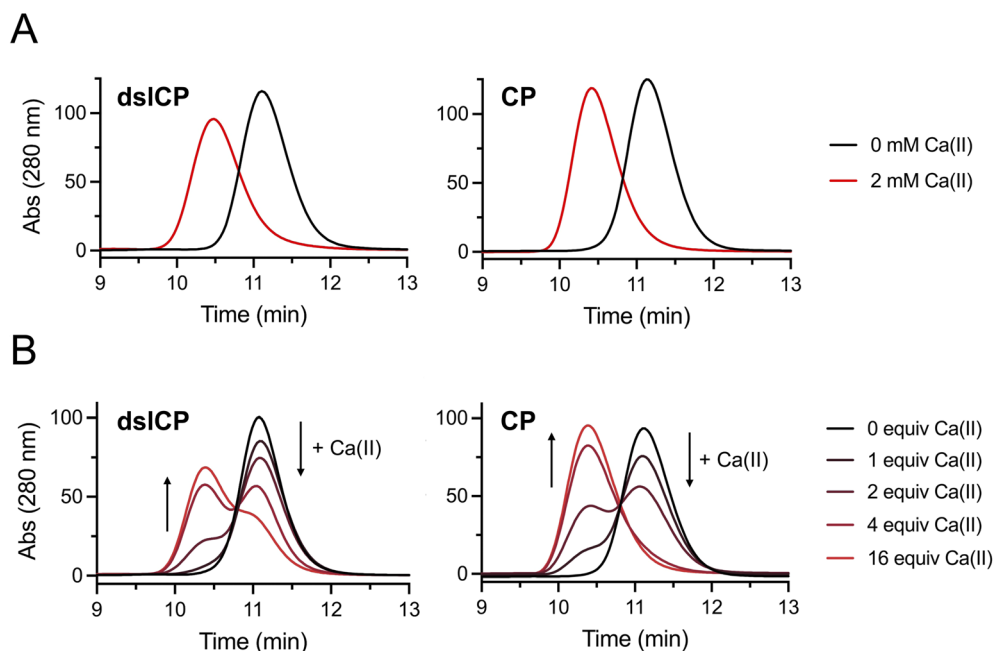


Fig. 3 dslCP and CP form heterotetramers in the presence of excess Ca(II) ions. (A) Analytical SEC traces of 100 μM dslCP (left) and CP (right) in the presence of 0 or 2 mM Ca(II) in the running buffer. (B) Analytical SEC traces of 80 μM dslCP (left) and CP (right) following incubation with varying equivalents of Ca(II) and no Ca(II) added to the running buffer. Molecular weight standards used for calibration are shown in Fig. S12. Table S9 reports peak elution volumes and corresponding molecular weights.

and CP-Ser in three different growth media that have been employed in studies of CP. CDM is a chemically defined medium that was originally described for *Staphylococcus aureus* growth⁴⁶ and that we have modified with defined metal concentrations for studies of CP.³¹ Tris : TSB is a rich medium and a mixture (62 : 38) of Tris buffer and tryptic soy broth (TSB) that has been employed in many studies examining the consequences of metal sequestration by CP and other S100 proteins on bacterial pathogens.^{28,30,32,33,47–52} Lastly, Tris : YPD (68 : 32) contains yeast-peptone-dextrose (YPD) medium for fungal growth. Each medium was supplemented with Ca(II) to mimic extracellular Ca(II) levels (1 mM for CDM; 2 mM for Tris : TSB and Tris : YPD). We treated each medium with 15 μM protein (30 $^{\circ}\text{C}$, 24 h, 150 rpm), separated the protein-bound and -unbound fractions by spin filtration (Fig. S13–S15), and quantified unbound metal levels (Mn, Fe, Ni, Cu, Zn) in the filtrate by inductively coupled plasma mass spectrometry (ICP-MS). The resulting data showed that dslCP depleted multiple metals from each microbial growth medium (Fig. 4). For instance, treatment of CDM with dslCP afforded significant decreases in metal concentrations, with a $\sim 90\%$ decrease in Mn, Ni, Cu and Zn and a $\sim 80\%$ decrease in Fe levels. Notably, comparison of metal depletion by dslCP, CP and CP-Ser demonstrated that dslCP depletes metals from CDM to a comparable extent as CP and CP-Ser. The same general trends were observed for Tris : TSB and Tris : YPD, in which dslCP treatment resulted in depletion of Mn, Fe, Ni, Cu and Zn to similar levels as CP and CP-Ser treatment (Fig. 4). Overall, these results indicated that formation of the intradimer disulfide bond has a negligible effect on the metal-depleting activity of CP and provided motivation for examining the antimicrobial activity of dslCP.

dslCP possesses broad-spectrum antimicrobial activity

We determined whether dslCP exhibits antimicrobial activity using a panel of seven clinically relevant microbial species, including the Gram-positive bacterial pathogen *S. aureus* USA300 JE2, the Gram-negative bacterial pathogens *Escherichia coli* CFT073, *Klebsiella pneumoniae* ATCC 13883, *Salmonella enterica* IR715, *Acinetobacter baumannii* ATCC 17978 and *Pseudomonas aeruginosa* PA14, and the single-celled opportunistic fungal pathogen *Candida albicans* SC5314 (Table S10). These organisms were chosen because they have been the subjects of prior studies focused on CP and nutritional immunity,^{3,32,53–55} and because they encompass a range of metal requirements.^{56–62} We performed antimicrobial activity assays by monitoring growth over time for cultures treated with dslCP, CP, or CP-Ser in CDM and Tris : TSB for the six bacterial species and in Tris : YPD for *C. albicans*. We observed that dslCP exhibited antimicrobial activity against all microbes tested across different medium conditions, and this activity was generally comparable to the growth inhibition caused by CP or CP-Ser treatment (Fig. 5 and S16–S18). Thus, these results indicate that the intradimer disulfide bond has negligible consequence for antimicrobial activity against the selected pathogens.

When examining the antimicrobial activity data, we noted some medium-dependent effects. For instance, *S. aureus* growth was inhibited to a greater extent in Tris : TSB than CDM. The data for *A. baumannii* indicated differences in antimicrobial activity between protein variants that were dependent on the growth medium. *A. baumannii* was equally susceptible to all three proteins in CDM, but varying degrees of



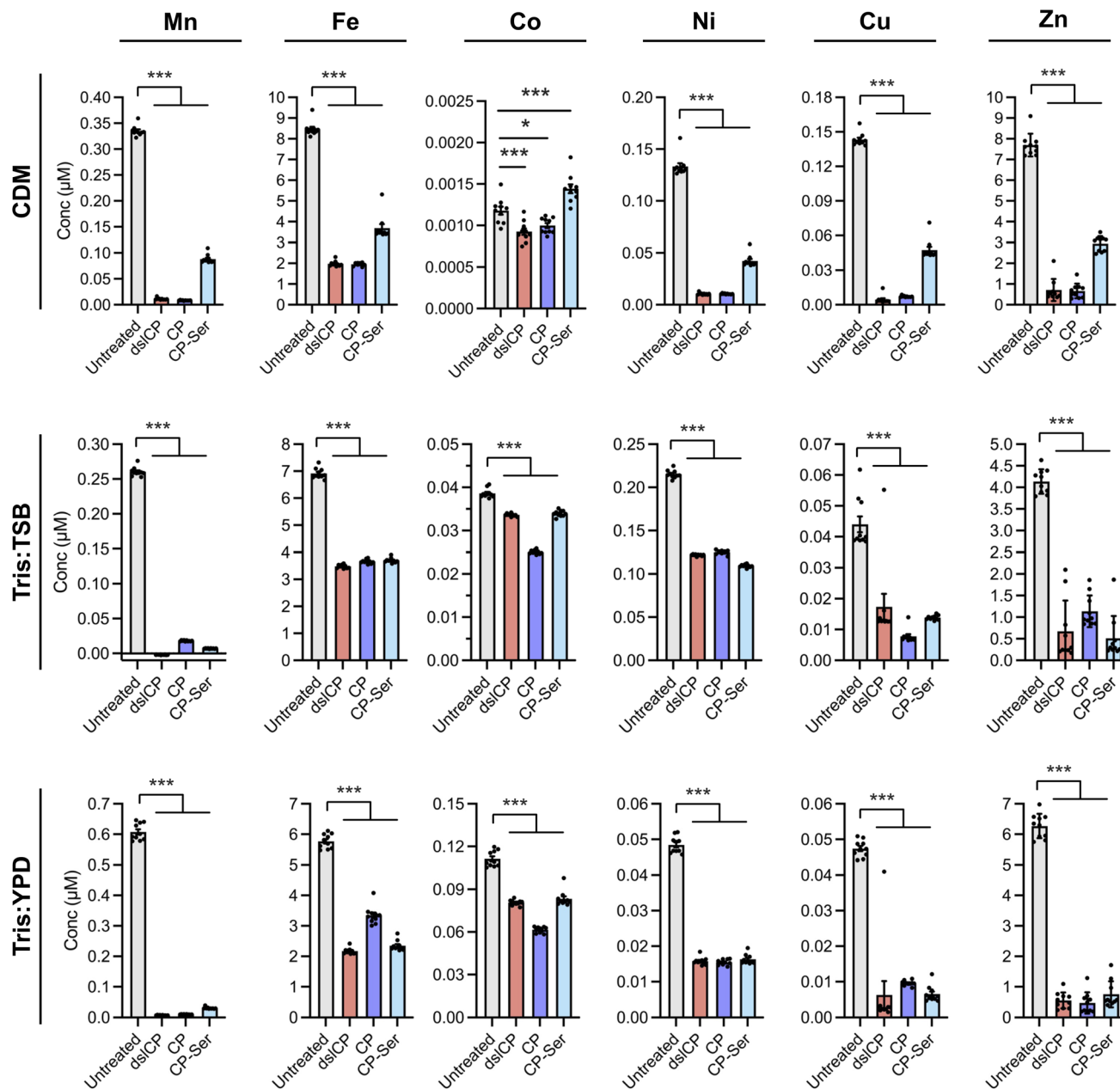


Fig. 4 dslCP depletes transition metals from microbial growth media. Metal depletion profiles of CDM (top), Tris : TSB (middle), and Tris : YPD (bottom) by dslCP, CP and CP-Ser. Media were incubated with or without 15 μM protein for 24 h at 30 $^{\circ}\text{C}$ and 150 rpm, filtered, and tested for metal content by ICP-MS. Samples of CP-treated media were supplemented with 5 mM DTT prior to incubation. All values are reported as mean \pm s.e.m.; $n = 10$ for all samples. Statistical significance was assessed by Welch's two-sample t -test. * $p < 0.05$, *** $p < 0.001$. In CDM samples, Co concentrations were near the ICP-MS detection limit.

growth inhibition was observed for this organism when the assays were performed in Tris : TSB, with dslCP displaying the weakest antimicrobial activity. Of the species included in the panel, *C. albicans* was the most sensitive to treatment with the three proteins; it failed to grow in the presence of all three protein variants under the conditions tested. This result is expected based on prior studies of the antifungal activities of CP^{3,4,34,63-69} and CP-Ser³⁵ and the Zn(II)-sequestering protein S100A12,⁴⁸ and the high metabolic Zn requirement exhibited by *C. albicans*.^{70,71}

dslCP treatment elicits siderophore production by diverse bacterial pathogens

We reasoned that the metal-depletion profile and broad-spectrum antimicrobial activity of dslCP were strong indicators of its ability to sequester metal nutrients from microbial pathogens. To further investigate this notion, we focused on bacterial siderophore production, which is a canonical Fe-starvation response and provides a means to probe for Fe withholding. We quantified siderophore production by five bacterial pathogens following treatment with dslCP, CP, and



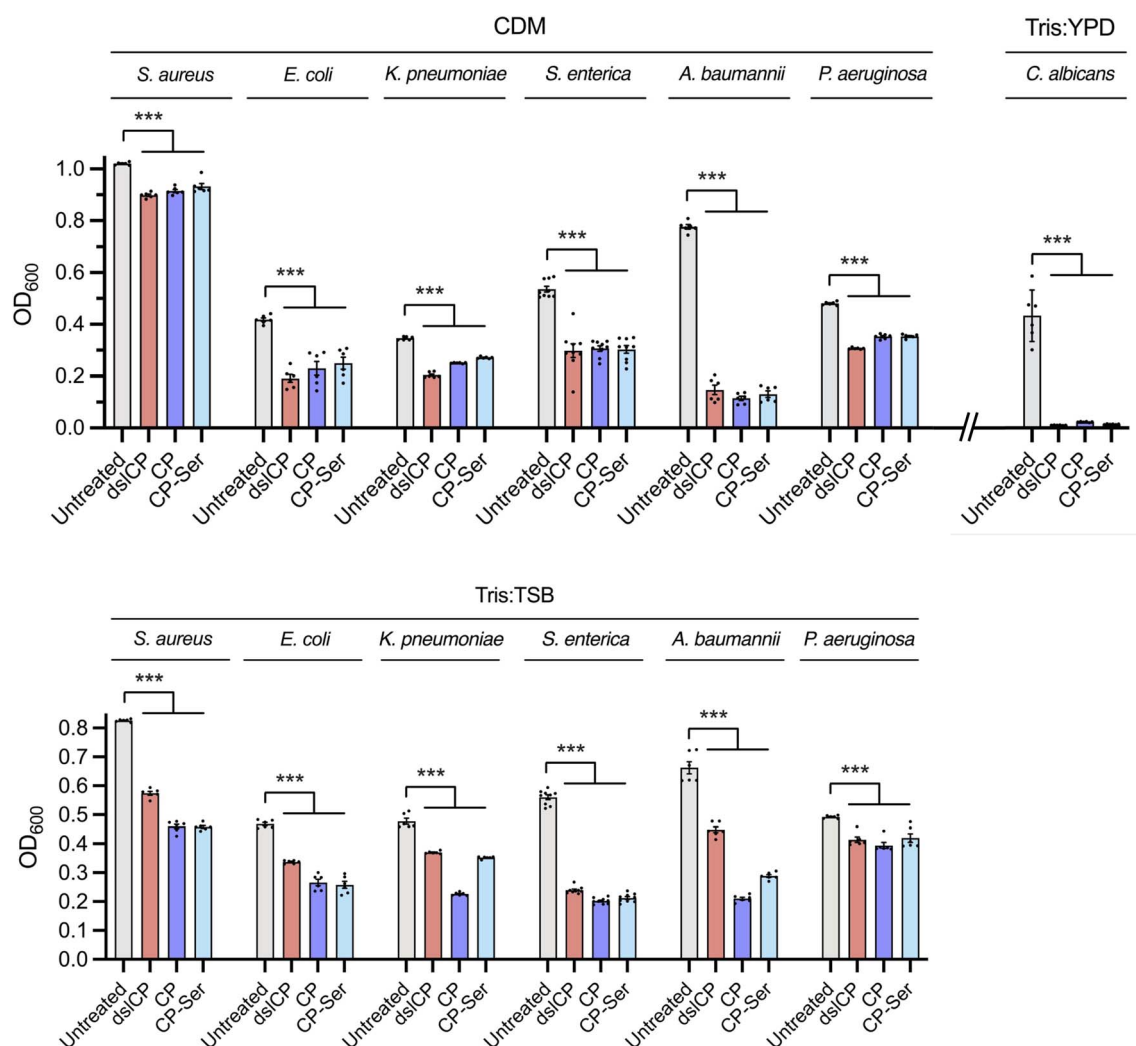


Fig. 5 dslCP exhibits broad-spectrum antimicrobial activity. OD₆₀₀ values are reported for each species following 12 h of growth in CDM, Tris : TSB or Tris : YPD. Species were grown at 37 °C in the presence of $\pm 10 \mu\text{M}$ dslCP, CP or CP-Ser. For *C. albicans*, OD₆₀₀ is reported after 22 h of growth at 37 °C. All values are reported as mean \pm s.e.m., $n = 6$ (*S. enterica*: $n = 9$). Statistical significance was assessed by Welch's two-sample *t*-test. *** $p < 0.001$.

CP-Ser by determining siderophore levels in culture supernatants using the universal CAS assay.^{72–74} When *S. aureus*, *E. coli*, *S. enterica*, *A. baumannii* and *P. aeruginosa* were treated with $15 \mu\text{M}$ dslCP for 8 h, the measured siderophore content in all five culture supernatants was significantly greater than that of the untreated controls and comparable to that of CP or CP-Ser treated cultures (Fig. 6 and S19). These results indicated that dslCP treatment induced iron-starvation responses in these bacterial pathogens, presumably by sequestering Fe(II) from the assay medium and attenuating bacterial iron uptake. The assay was also attempted for *K. pneumoniae* supernatants, but siderophore quantification was complicated by precipitation of the dye complex and a lack of naked-eye observable color differences between protein-treated and untreated culture supernatants. Despite this complication, our overall results from the panel of microbes indicate that dslCP is capable of eliciting iron-starvation responses in diverse bacterial pathogens.

dslCP exhibits proteolytic instability

Two prior studies examining the protease susceptibility of mixtures that contained oxidized CP species indicated that dslCP is more susceptible to proteolytic degradation than CP under conditions of excess Ca(II).^{19,20} This observation was somewhat surprising given the common role of disulfide bonds as “molecular staples” that stabilize secondary and tertiary structures. Because neither study analyzed an isolated sample of dslCP, we revisited these proteolytic susceptibility experiments using purified dslCP. We evaluated the stability of dslCP towards digestion by two serine proteases, human neutrophil elastase (HNE) and trypsin. These proteases were employed in the prior work and are biologically relevant because they co-localize with CP *in vivo*: HNE is present at sites of infection and neutrophil infiltration,⁷⁵ whereas trypsin is abundant in the gastrointestinal tract.⁷⁶ For comparison and as controls, we included CP-Ser and its I60E variant in these assays; the Ca(II)-



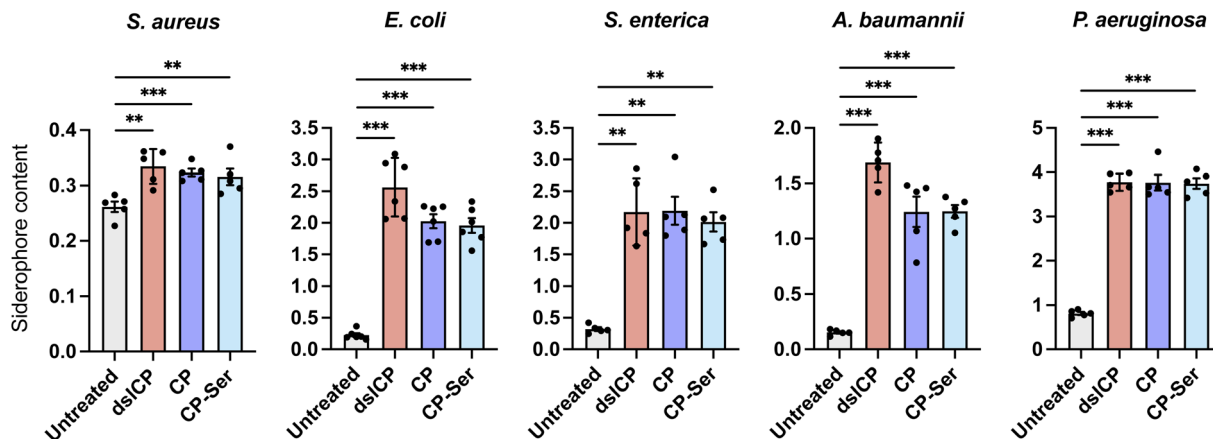


Fig. 6 Siderophore content of bacterial supernatants following 8 h of growth at 37 °C in CDM with 15 μ M dsICP, CP, or CP-Ser treatment. The plotted values are the siderophore content of culture supernatants calculated based on the A_{630} of the samples and the media-only reference. Values were normalized to the OD_{600} of the cultures. All values are reported as mean \pm s.e.m.; $n = 5$ for all samples except *E. coli* ($n = 6$). Statistical significance was assessed by pairwise comparisons (Welch's two-sample t -test) between each individual treatment group and the untreated control. No statistical comparisons were made between different protein treatment groups. ** $p < 0.01$, *** $p < 0.001$.

bound CP-Ser heterotetramer exhibits protease resistance while I60E, which does not undergo Ca(II)-dependent tetramerization and thus is a Ca(II)-bound heterodimer, exhibits enhanced proteolytic susceptibility.²⁷ Moreover, we included samples incubated with 1 equiv of Mn(II) because Mn(II) binding causes the I60E variant to self-associate and form a protease-resistant heterotetramer under these assay conditions.²⁷

Analytical HPLC analyses of the protease digests revealed that dsICP was readily degraded by both HNE and trypsin (Fig. 7A and S20–S28). This observation is consistent with the two prior studies that analyzed the proteolytic susceptibility of CP mixtures containing dsICP.^{19,20} Moreover, the protease degradation time-course data for CP-Ser and I60E reproduced prior findings and revealed that the degradation rate of dsICP was intermediate between that of CP-Ser and I60E (Fig. 7B). Introduction of 1 equiv of Mn(II) into each sample resulted in a near-complete protection of all three proteins against digestion (Fig. 7A and B). CP-Ser remained resistant to digestion regardless of Mn(II) addition, consistent with its known ability to form a Ca(II)-bound, protease-resistant heterotetramer. In the case of I60E, protection from proteolysis upon addition of Mn(II) was shown in an earlier study to be a result of Mn(II)-induced tetramerization that shielded cut sites from protease access.²⁷ However, tetramerization alone cannot explain Mn(II)-dependent protection in dsICP, as dsICP already exists as a tetramer under the excess Ca(II) conditions of the assay (Fig. 3A). Thus, we sought alternative explanations for the behavior of dsICP. We reasoned that two underlying processes could explain its proteolytic susceptibility as well as the protease resistance observed in the presence of Ca(II) and Mn(II). One possible explanation is that in the presence of excess Ca(II) alone, dsICP exists as a rapidly interconverting mixture of Ca(II)-bound dimers and tetramers that is not resolved by analytical SEC. Mn(II) binding, presumably to the His₆ site of dsICP, causes the dynamic equilibrium to shift in favor of the heterotetrameric species, which is protease resistant.²⁷ We previously found this

scenario to be at play during studies of Met-oxidized CP-Ser.¹⁹ Methionine oxidation caused Ca(II)-bound CP-Ser to switch from a heterotetrameric population to an interconverting system, which resulted in increased proteolytic susceptibility due to degradation of the heterodimeric species. Mn(II) binding to Met-oxidized CP-Ser caused the protein to tetramerize and become resistant to degradation by trypsin. A second plausible explanation is that intradimer disulfide bond formation sensitizes the protein scaffold to proteolytic degradation regardless of oligomeric state by altering the protein fold to expose one or more cut sites that are not accessible in Ca(II)-bound CP. This effect is mitigated by Mn(II) binding, perhaps resulting from tighter packing or other conformational change in the region near the cut site(s).

In order to distinguish between these two possibilities, we employed sedimentation velocity analytical ultracentrifugation (SV-AUC) to further elucidate the self-association properties of dsICP and, specifically, to probe whether Ca(II)-bound dsICP is an interconverting or non-interconverting system.^{19,77,78} We determined sedimentation coefficients for dsICP and CP-Ser in the absence of Ca(II) as well as in the presence of excess Ca(II) (550 μ M or 2 mM), with or without 1 equiv of Mn(II) (Fig. 7C and S29–S32, Tables S11–S13). The SV-AUC analysis demonstrated that both apo CP-Ser and apo dsICP existed as dimers with sedimentation coefficients of 2.1 S, corresponding to molecular weights of 22.9 and 23.6 kDa, respectively (Table S12). Addition of 20 equiv of Ca(II) (550 μ M) was sufficient to induce complete tetramerization in both proteins, yielding sedimentation coefficients of 3.4 S and molecular weights of 44.4 kDa for CP-Ser and 43.0 kDa for dsICP. Under physiological levels of Ca(II) (2 mM), CP-Ser retained its 3.4 S sedimentation coefficient (45.2 kDa). By contrast, dsICP shifted to 3.6 S while retaining a similar molecular weight (47.4 kDa), indicative of the formation of Ca(II)-bound heterotetramers with altered hydrodynamic radii. Both CP-Ser and dsICP shifted to a larger S value upon Mn(II) addition (3.6 S and 3.8 S, respectively, corresponding to 46.2



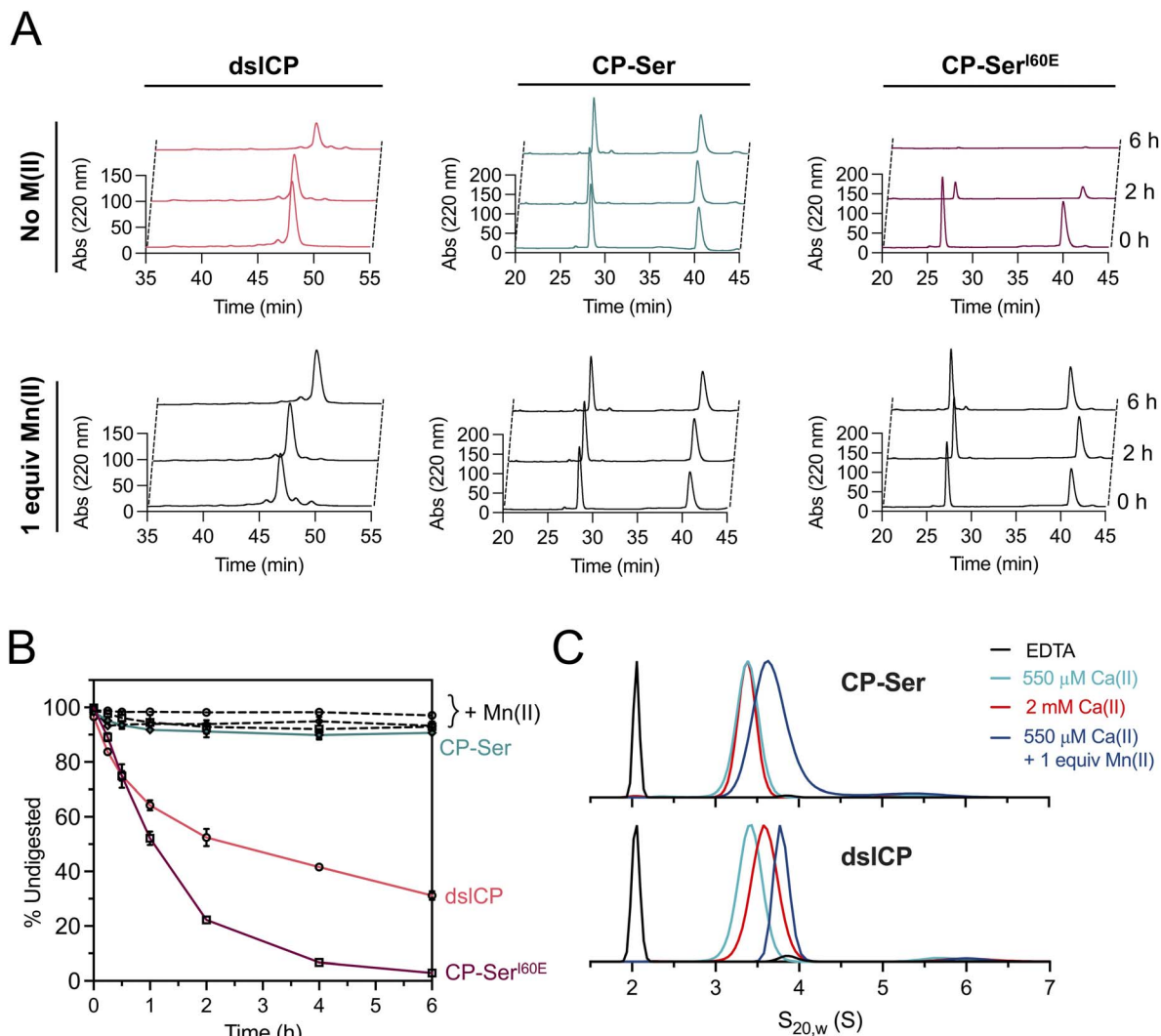


Fig. 7 dsICP exhibits increased proteolytic susceptibility to HNE. (A) HPLC time-course stack plots for dsICP, CP-Ser and CP-Ser^{I60E} treated with 2.5 μM HNE for 0–6 h in the presence and absence of 1 equiv Mn(II). (B) Quantification of the traces in A (mean ± s.e.m., $n = 3$). The + Mn(II) controls are shown with dashed grey lines. (C) SV-AUC analysis of CP-Ser and dsICP. Samples (27.5 μM) were analyzed in the apo state or after incubation with 20 equiv Ca(II) (550 μM), physiological Ca(II) (2 mM), and/or 1 equiv Mn(II) as indicated. Plots were normalized to a maximum peak height of 1 (refer to Fig. S37 for unnormalized plots).

and 49.0 kDa). We note that a second, independent SV-AUC run (Fig. S33–S36) yielded similar results, albeit dsICP displayed an increased tendency to form higher-order oligomers in the presence of Ca(II) or Mn(II). The different behavior observed is likely a result of slight variations between dsICP preparations, although the possibility of a metal contamination in the second run cannot be excluded. Of relevance to understanding the proteolytic susceptibility of dsICP, the +Ca(II) samples contained no measurable dimeric population of dsICP, and the tetramer peak did not shift toward lower S values. Consequently, the SV-AUC experiments in the presence of Ca(II) provide no evidence for dsICP being an interconverting system. Thus, these results indicate that the increased susceptibility of dsICP to digestion by HNE and trypsin is unlikely to result from an altered dimer–tetramer equilibrium, but instead from structural changes that increase protease accessibility to one or

more cut sites. Future studies are warranted to identify the cut site(s) as well as the structural changes induced by disulfide bond formation that may increase proteolytic susceptibility.

Redox properties of the S100A8–S100A9 disulfide bond

To evaluate the redox properties of the Cys42–Cys3 disulfide bond in dsICP and whether it could undergo reversible reduction under biologically relevant redox conditions, we determined its midpoint potential (E_m). We incubated dsICP in buffers with varying redox potentials achieved using defined ratios of DTT_{ox}:DTT_{red} (–225 to –196 mV, see SI Discussion), in the presence or absence of 3 mM Ca(II) at pH 7.0 (37 °C, 24 h, anaerobic). We subsequently analyzed the samples by SDS-PAGE to assess the redox speciation of the protein. The data revealed that in both the absence and presence of excess Ca(II), dsICP was predominantly oxidized when incubated in buffers



with more positive redox potentials and predominantly reduced following incubation in buffers with more negative redox potentials (Fig. 8A). As expected for a redox transition, mixtures of oxidized and reduced species were observed near the midpoint. However, even at the most oxidizing potentials examined, a persistent fraction of reduced dslCP remained, preventing the data from approaching the expected upper plateau for a simple two-state, two-electron Nernst transition (Fig. S38A and B). We thus fit the data using a four-parameter logistic function that allows the upper and lower asymptotes to vary (see SI Discussion; also see Fig. S38C, D, Tables S14 and S15). Consistent with visual estimates, this fitting procedure afforded E_m values of -213.5 ± 1.0 mV and -215.1 ± 2.4 mV for apo and Ca(II)-bound dslCP, respectively (Fig. 8B and C). These data indicated that Ca(II) binding had a negligible effect on the E_m value of the intradimer disulfide bond, and that this value falls within the range typically associated with redox-active disulfides (Table S16).

We noted that the determined E_m values for dslCP were more positive than that of thioredoxin (Trx), a cellular redox regulator that operates alongside the glutathione system (Fig. 9A).^{79–81} Trx operates in conjunction with thioredoxin reductase (TrxR) and NADPH to reduce disulfides to their constituent cysteines.⁸² Trx possesses many homologs across diverse species, and the human protein displays a midpoint potential of approximately -230 mV.⁷⁹ Because CP is a human host-defense protein, we considered the possibility that dslCP could be a substrate for the human Trx system. To test this notion, we mixed apo dslCP with catalytic amounts of human Trx, rat liver TrxR, and excess NADPH at pH 7.0 and monitored the proportion of oxidized and reduced CP species in the reaction mixture over time by Western blot (Fig. 9B, and S42). We observed quantitative conversion of dslCP to CP in less than 10 min, as evidenced by the detection of S100A8_{red} and S100A9_{red}, demonstrating that

the Trx system readily accepted dslCP as a substrate to afford CP (Fig. S40). Control reactions in which individual components of the Trx system were omitted showed no detectable reduction of dslCP (Fig. S41).

Next, we examined the consequences of Ca(II) addition on dslCP reduction by the Trx system. When excess Ca(II) was included in the reaction, reduction of the intradimer disulfide bond occurred but was relatively slow compared to the reduction in the absence of added Ca(II) (Fig. 9B and C). The $t_{1/2}$ of 2.4 min for apo dslCP reduction increased to 74.9 min when excess Ca(II) was added to the reaction mixture (Fig. S43). This result indicated that the Trx system reduces the intradimer disulfide bond less efficiently when dslCP is in its Ca(II)-bound heterotetrameric form, despite this species having the same E_m value as the apo protein. We note that because Ca(II) does not inhibit the thioredoxin system,^{42,83} the observed decrease in the reduction rate is unlikely to arise from direct inhibition of the protein machinery. Instead, it is possible that Ca(II)-induced tetramerization or other Ca(II)-induced conformational changes within dslCP decrease the accessibility or reactivity of the disulfide bond.

To study the effect of transition-metal binding on dslCP reduction by the Trx system, we pre-incubated dslCP with 1 equiv of Mn(II) and excess Ca(II), which resulted in only a moderate decrease in reduction rate compared to the +Ca(II) condition. By contrast, pre-incubation with 1.9 equiv of Zn(II) and excess Ca(II) substantially slowed disulfide bond reduction, and dslCP remained the predominant species throughout the reaction (Fig. 9B and C). These M(II) equivalents were selected because CP has one high-affinity Mn(II) site (His₆)^{29,36} and two high-affinity Zn(II) sites (His₆ and His₃Asp).^{28,35} The origin of the stabilizing effect of Zn(II) binding against reduction of dslCP by thioredoxin is unclear. It is possible that metal binding to the His₃Asp site alters the three-dimensional shape of dslCP in

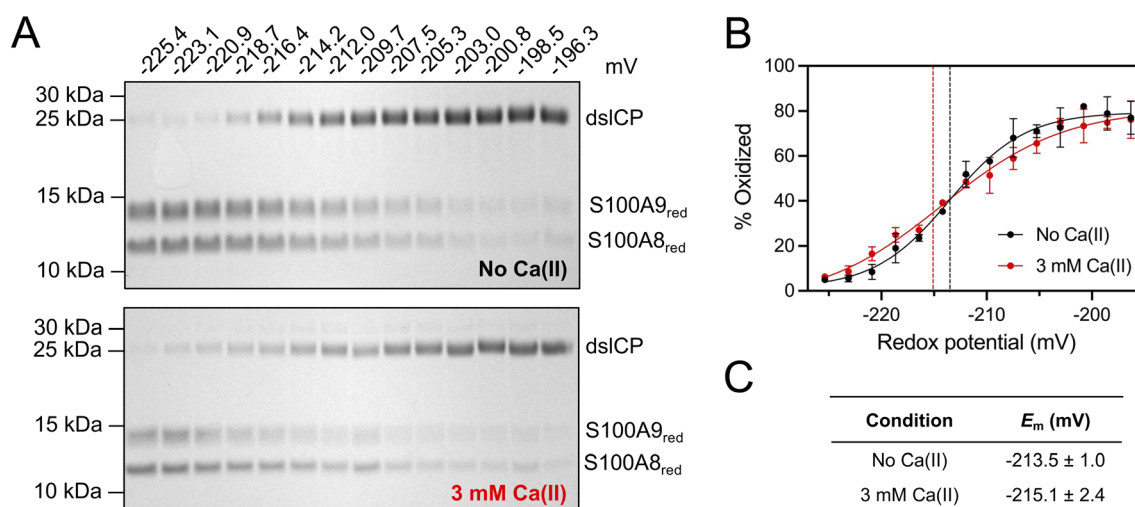


Fig. 8 Midpoint potential value determination for dslCP in the absence and presence of excess Ca(II) ions. (A) Representative SDS-PAGE gels of dslCP incubated with varying ratios of DTT_{ox} : DTT_{red} and ± 3 mM Ca(II). Samples were incubated for 24 h at 37 °C under anaerobic conditions. (Protein concentration: 20 μ M; [DTT_{ox}] + [DTT_{red}] = 100 mM). (B) Quantification of the gels from panel A (mean \pm s.e.m.; $n = 3$). The dashed vertical lines indicate the midpoint based on the fit to a four-parameter logistic model (see SI Discussion). (C) Computed E_m values in the presence and absence of excess Ca(II).



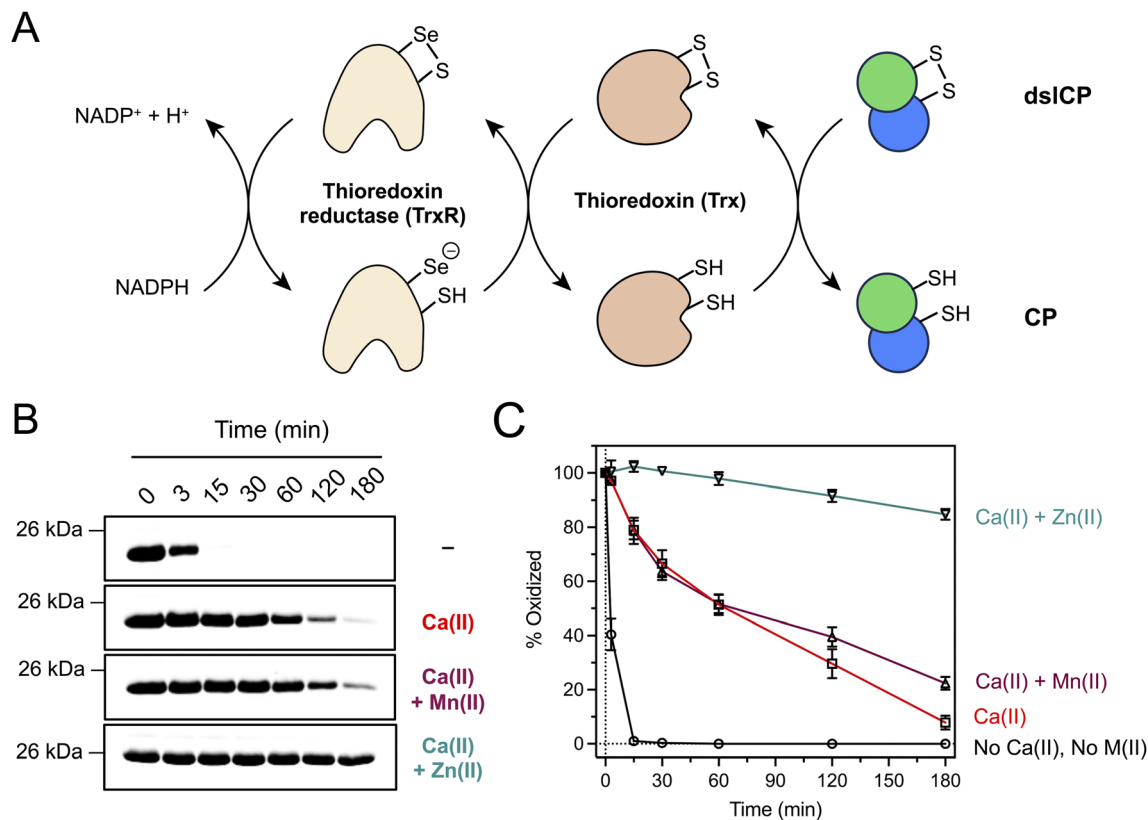


Fig. 9 dslCP is a substrate of the Trx system. (A) Trx reduces disulfide bonds in proteins and is kept catalytically active by thioredoxin reductase (TrxR) and NADPH. As in Fig. 1, S100A8 is shown in green and S100A9 in blue. (B) α -S100A9 Western blots depicting the change in dslCP levels over time in the presence of Trx (2.5 μ M), TrxR (0.05 μ M) and NADPH (2.5 mM). Proteins were incubated with either no Ca(II) or 2 mM Ca(II), and either 1 equiv Mn(II) or 1.9 equiv Zn(II) as indicated. (C) Quantification of the Western blots in panel B (mean \pm s.e.m.; $n = 3$).

a manner that impairs thioredoxin access to the intradimer disulfide bond. Alternatively, metal binding at the His₃Asp site may alter the midpoint potential of the disulfide bond by changing the local electrostatic environment or conformational dynamics around the Cys residues. Finally, we cannot exclude a potential role of Zn(II) in templating higher-order oligomerization, which has been observed for CP^{84,85} and may impede Trx accessibility.^{84,85}

In summary, our redox characterization of dslCP indicated that this protein behaves as a redox-responsive species. Its midpoint potential (−213 mV) falls within the range characteristic of reversible disulfides, consistent with the apo protein being readily reduced by the Trx system. At the same time, studies with the Trx system indicate that Ca(II) and Zn(II) binding perturb the ability of Trx to reduce the intradimer disulfide bond.

Discussion

In this work, we examined the biochemical and functional consequences of intradimer disulfide bond formation in CP. Our findings show that the disulfide-linked form, dslCP, retains many of the properties of CP: it is highly α -helical, undergoes Ca(II)-dependent tetramerization, depletes microbial growth media of nutrient transition metals, exerts broad-spectrum

antimicrobial activity, and induces siderophore production by diverse bacterial pathogens. These findings indicate that dslCP has the capacity to participate in nutritional immunity and provide motivation for future studies of its biological coordination chemistry and impacts on microbial physiology. Our study also shows that dslCP and CP differ in some profound ways. Notably, dslCP appears to require more Ca(II) equivalents to fully tetramerize. Further investigations are necessary to understand the biophysical basis of this observation and determine whether it has any functional consequences *in vivo*. We also found that dslCP is more susceptible to proteolysis by host proteases. This feature was apparent in two prior studies using protein mixtures.^{19,20} Formation of the intradimer disulfide bond undoubtedly has structural consequences that require elucidation.

Collectively, our data and those of others support a model in which dslCP forms following neutrophil release of CP into the extracellular space. The neutrophil cytoplasm is reducing, with a reported potential of −318 mV for a neutrophil at rest and −264 mV upon activation.⁸⁶ In contrast, the extracellular space is generally more oxidizing,⁸⁷ and can become even more oxidizing as a result of the neutrophil oxidative burst.^{1,2} Disulfide bond formation within CP may occur before, concurrently with, or after Ca(II) or M(II) binding. Regardless of the order of these events, our data indicate that Ca(II)-bound dslCP



exists as a heterotetramer. We anticipate that dslCP has multiple possible fates in the extracellular space. dslCP may participate in the metal withholding response by sequestering available divalent transition-metal ions, and this binding event affords protease resistance similar to what we previously proposed for methionine-oxidized CP.¹⁹ Because the intradimer disulfide bond in dslCP sensitizes the Ca(II)-bound protein to proteolytic attack, in the absence of a bound transition-metal ion the protein can be readily degraded by extracellular proteases. This work expands on our prior study of CP oxidation, where we proposed that the enhanced proteolytic susceptibility of the methionine-oxidized and disulfide-bonded forms may serve a physiological role by promoting the clearance of extracellular CP and thereby attenuating CP-mediated pro-inflammatory signaling (Fig. 10).^{19,88–91} Meanwhile, by targeting only the apo and Ca(II)-bound protein, this pathway avoids metal release from M(II)-bound dslCP, which would counter its involvement in nutritional immunity.

Although disulfide bonds are generally viewed as stabilizing, and thus the proteolytic susceptibility of dslCP may seem unusual,^{92–94} Cys oxidation triggering protein instability has precedent. For example, human angiotensinogen contains two highly conserved cysteine residues (Cys18/138) that form a redox-sensitive disulfide bond. This bond induces a major conformational change that exposes the N-terminal tail for proteolytic cleavage by the aspartyl protease renin.⁹⁵ This cleavage event initiates the production of angiotensin peptides that regulate blood pressure. Cys oxidation has also been found to trigger protein clearance. For instance, human serum albumin contains a single, redox-active cysteine (Cys34) which usually exists in its reduced form. Oxidation of Cys34 to either a mixed disulfide or a sulfinic/sulfonic acid results in conformational loosening of domain I.⁹⁶ This conformational change reduces the affinity of serum albumin for its ligands⁹⁷ and promotes recognition by hepatic scavenger receptors (*e.g.*, SR-A and CD36), ultimately leading to endocytosis and lysosomal degradation.⁹⁸

In the context of S100 proteins, disulfide bonding has been reported in a number of homologs including S100A2,^{99–101}

S100A4,^{102,103} S100A11 (S100C),^{104,105} S100A7,^{42,106} S100B,^{44,107} murine S100A8,⁴³ and murine S100A9.^{108,109} The reported consequences of this post-translational modification are diverse, affecting processes as varied as subcellular localization, protein oligomeric state, ligand interactions, and antimicrobial activity.^{42,99,100,103,106,109} For the S100A2 homodimer, the formation of intra- and inter-dimeric disulfide bonds alters its interaction with target proteins such as p53 and regulates its movement between the cytoplasm and the nucleus, serving as a sensor for oxidative stress in the cell.^{99,100,110} In S100A7, intradimer disulfide bond formation enhances structural stability, Zn(II) sequestration, and antimicrobial activity.⁴² In the murine S100A9 homodimer, an intrasubunit disulfide bridge between Cys91 and Cys111 stabilizes the C-terminal tail in a rigid conformation, creating an additional Zn(II) binding site.¹⁰⁹ The rigidification of the C-terminal tail in the murine homolog serves to tether the flexible C-terminus, which can also be achieved *via* hydrophobic interactions as evidenced by a study of human CP.²⁵ Despite the extensive studies probing the functional consequences of disulfide bonding in S100 proteins, whether this PTM affects the proteolytic susceptibility and lifetime of other S100 proteins remains unclear and represents a worthwhile topic for future investigation.

Concluding this discussion, we note the remarkable combined use of Ca(II) ions and disulfide bonds in the extracellular space and endoplasmic reticulum, which has been the focus of studies across several unrelated systems that we highlight here. First, our group studied disulfide bond formation in S100A7 and reported that Ca(II) binding lowers the midpoint potential of the S100A7 intradimer disulfide bond, making the Ca(II)-bound oxidized form more resistant to reduction and attenuating the ability of the Trx system to convert S100A7_{ox} to S100A7_{red}.⁴² In the current work, we observed a similar effect for dslCP in which the Ca(II)-bound protein was less readily reduced by the Trx system, although this result was not reflected in a depression of the E_m value under conditions of excess Ca(II) (Fig. 8 and 9). Second, studies of collagen assembly revealed a relationship between Ca(II) binding and disulfide formation,

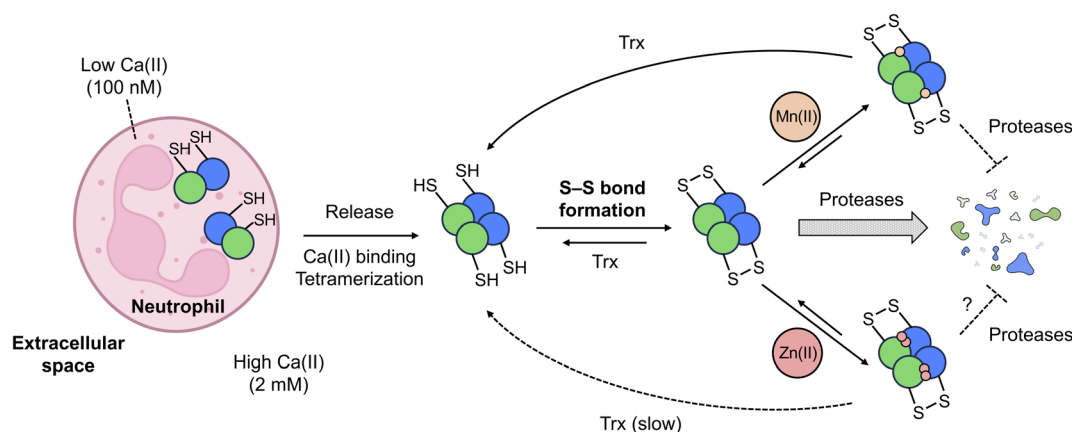


Fig. 10 Proposed model for the effect of disulfide bond formation on CP speciation and persistence. The disulfide bond is formed in the extracellular space as a result of the oxidizing environment and reactive oxygen species. The reactivity of dslCP towards proteases and the thioredoxin system are highlighted. The disulfide bond is depicted forming after tetramerization and prior to metal binding; however, the order of these events may differ (see text for details). Ca(II) ions are omitted for clarity. The neutrophil schematic was created with BioRender.



whereby Ca(II) binding precedes disulfide bond formation and templates maturation of the collagen triple helix.¹¹¹ Third, studies of mammalian transglutaminase-2 (TG2) revealed that disulfide bonding and Ca(II) binding had opposing effects on enzymatic activity: Ca(II) binding activates TG2 by promoting its catalytically competent conformation, whereas formation of the Cys370–Cys371 disulfide bond inhibits its activity.^{112–114} Taken together, these examples cover proteins that have diverse functions but all use both Ca(II) and disulfide bonding in some way to modulate their structure and regulate their activity and stability. These observations raise the possibility that interplay between Ca(II) ions and disulfide bonds plays a role in shaping protein structure and function in oxidizing environments such as the extracellular space and endoplasmic reticulum.

Conclusion

This study provides initial insights into how intradimer disulfide bond formation in CP impacts the biochemical properties and function of this remarkable metal-sequestering protein. CP speciation has largely been conceptualized from the perspectives of self-association and divalent cation binding. However, recent studies, including ours, make it increasingly apparent that PTMs require consideration and integration into our understanding of how CP functions in innate immunity and host defense. This work considered disulfide bond formation in isolation; however, it is likely that this oxidative PTM occurs concurrently with methionine oxidation *in vivo* due to the neutrophil oxidative burst. Thus, ascertaining the consequences of multiple PTMs should be informative. We anticipate that future investigations will continue to examine PTMs—individually and in combinations—and their effects on CP in metal sequestration and beyond.

Author contributions

Aurelio Mollo: conceptualization, methodology, validation, formal analysis, investigation, writing – original draft, writing – review & editing, visualization. Emma Y. Cool: conceptualization, methodology, validation, formal analysis, investigation, writing – original draft, writing – review & editing, visualization. Bahar Sakar: methodology, validation, investigation, writing – review & editing. Kushol Gupta: methodology, formal analysis, investigation, data curation, writing – review & editing, visualization. Elizabeth M. Nolan: conceptualization, resources, supervision, project administration, funding acquisition, writing – review & editing.

Conflicts of interest

There are no conflicts to declare.

Data availability

The data supporting this article are available within the article and its supplementary information (SI). Supplementary information: experimental procedures, a supplementary discussion,

and additional figures and tables. See DOI: <https://doi.org/10.1039/d6sc02543a>.

Acknowledgements

This work was supported by the NIH R01 GM118695 to EMN. EC was supported by the Stephen J. Lippard (1965) Fund. BS was supported by the MIT Summer Research Program in Biology. We thank Dr Bogdan Fedeles for assistance with ICP-MS measurements. KG acknowledges support from the Johnson Research Foundation and NIH Shared Instrumentation Grant S10-OD018483.

References

- 1 C. C. Winterbourn, A. J. Kettle and M. B. Hampton, *Annu. Rev. Biochem.*, 2016, **85**, 765–792.
- 2 J. El-Benna, M. Hurtado-Nedelec, V. Marzaioli, J.-C. Marie, M.-A. Gougerot-Pocidallo and P. M.-C. Dang, *Immunol. Rev.*, 2016, **273**, 180–193.
- 3 M. Steinbakk, C.-F. Naess-Andresen, E. Lingaas, I. Dale, P. Brandtzaeg and M. K. Fagerhol, *Lancet*, 1990, **336**, 763–765.
- 4 P. G. Sohnle, C. Collins-Lech and J. H. Wiessner, *J. Infect. Dis.*, 1991, **164**, 137–142.
- 5 B. D. Corbin, E. H. Seeley, A. Raab, J. Feldmann, M. R. Miller, V. J. Torres, K. L. Anderson, B. M. Dattilo, P. M. Dunman, R. Gerads, R. M. Caprioli, W. Nacken, W. J. Chazin and E. P. Skaar, *Science*, 2008, **319**, 962–965.
- 6 E. M. Zygiel and E. M. Nolan, *Annu. Rev. Biochem.*, 2018, **87**, 621–643.
- 7 J. Edgeworth, M. Gorman, R. Bennett, P. Freemont and N. Hogg, *J. Biol. Chem.*, 1991, **266**, 7706–7713.
- 8 S. Teigelkamp, R. S. Bhardwaj, J. Roth, G. Meinardus-Hager, M. Karas and C. Sorg, *J. Biol. Chem.*, 1991, **266**, 13462–13467.
- 9 M. J. Hunter and W. J. Chazin, *J. Biol. Chem.*, 1998, **273**, 12427–12435.
- 10 T. Vogl, J. Roth, C. Sorg, F. Hillenkamp and K. Strupat, *J. Am. Soc. Mass Spectrom.*, 1999, **10**, 1124–1130.
- 11 K. Strupat, H. Rogniaux, A. Van Dorsselaer, J. Roth and T. Vogl, *J. Am. Soc. Mass Spectrom.*, 2000, **11**, 780–788.
- 12 E. M. Nolan and J. J. Y. Peet, *BioMetals*, 2023, **36**, 817–828.
- 13 M. J. Raftery, Z. Yang, S. M. Valenzuela and C. L. Geczy, *J. Biol. Chem.*, 2001, **276**, 33393–33401.
- 14 L. H. Gomes, M. J. Raftery, W. X. Yan, J. D. Goyette, P. S. Thomas and C. L. Geczy, *Free Radic. Biol. Med.*, 2013, **58**, 170–186.
- 15 T. Cabras, M. Sanna, B. Manconi, D. Fanni, L. Demelia, O. Sorbello, F. Iavarone, M. Castagnola, G. Faa and I. Messina, *J. Proteomics*, 2015, **128**, 154–163.
- 16 N. J. Magon, R. Turner, R. B. Geary, M. B. Hampton, P. D. Sly and A. J. Kettle, *Free Radic. Biol. Med.*, 2015, **86**, 133–144.
- 17 J. M. Spraggins, D. G. Rizzo, J. L. Moore, K. L. Rose, N. D. Hammer, E. P. Skaar and R. M. Caprioli, *J. Am. Soc. Mass Spectrom.*, 2015, **26**, 974–985.



- 18 C. Martelli, V. Marzano, F. Iavarone, L. Huang, F. Vincenzoni, C. Desiderio, I. Messina, P. Beltrami, F. Zattoni, P. M. Ferraro, N. Buchholz, G. Locci, G. Faa, M. Castagnola and G. Gambaro, *J. Urol.*, 2016, **196**, 911–918.
- 19 J. R. Stephan, F. Yu, R. M. Costello, B. S. Bleier and E. M. Nolan, *J. Am. Chem. Soc.*, 2018, **140**, 17444–17455.
- 20 T. S. Hoskin, J. M. Crowther, J. Cheung, M. J. Epton, P. D. Sly, P. A. Elder, R. C. J. Dobson, A. J. Kettle and N. Dickerhof, *Redox Biol.*, 2019, **24**, 101202.
- 21 C. Dubois, D. Payen, S. Simon, C. Junot, F. Fenaille, N. Morel and F. Becher, *J. Proteome Res.*, 2020, **19**, 914–925.
- 22 T. S. Edwards, N. Dickerhof, N. J. Magon, L. N. Paton, P. D. Sly and A. J. Kettle, *J. Immunol.*, 2022, **208**, 979–990.
- 23 N. Dickerhof, L. V. Ashby, D. Ford, J. J. Dilly, R. F. Anderson, R. J. Payne and A. J. Kettle, *J. Biol. Chem.*, 2025, **301**, 108402.
- 24 S. Y. Lim, M. J. Raftery, J. Goyette and C. L. Geczy, *J. Biol. Chem.*, 2010, **285**, 14377–14388.
- 25 R. Silvers, J. R. Stephan, R. G. Griffin and E. M. Nolan, *J. Am. Chem. Soc.*, 2021, **143**, 18073–18090.
- 26 J. Adhikari, J. R. Stephan, D. L. Rempel, E. M. Nolan and M. L. Gross, *J. Am. Chem. Soc.*, 2020, **142**, 13372–13383.
- 27 J. R. Stephan and E. M. Nolan, *Chem. Sci.*, 2016, **7**, 1962–1975.
- 28 M. B. Brophy, J. A. Hayden and E. M. Nolan, *J. Am. Chem. Soc.*, 2012, **134**, 18089–18100.
- 29 J. A. Hayden, M. B. Brophy, L. S. Cunden and E. M. Nolan, *J. Am. Chem. Soc.*, 2013, **135**, 775–787.
- 30 T. G. Nakashige, B. Zhang, C. Krebs and E. M. Nolan, *Nat. Chem. Biol.*, 2015, **11**, 765–771.
- 31 T. G. Nakashige, E. M. Zygiel, C. L. Drennan and E. M. Nolan, *J. Am. Chem. Soc.*, 2017, **139**, 8828–8836.
- 32 S. M. Damo, T. E. Kehl-Fie, N. Sugitani, M. E. Holt, S. Rathi, W. J. Murphy, Y. Zhang, C. Betz, L. Hench, G. Fritz, E. P. Skaar and W. J. Chazin, *Proc. Natl. Acad. Sci. U. S. A.*, 2013, **110**, 3841–3846.
- 33 T. E. Kehl-Fie, S. Chitayat, M. I. Hood, S. Damo, N. Restrepo, C. Garcia, K. A. Munro, W. J. Chazin and E. P. Skaar, *Cell Host Microbe*, 2011, **10**, 158–164.
- 34 A. N. Besold, B. A. Gilston, J. N. Radin, C. Ramsomair, E. M. Culbertson, C. X. Li, B. P. Cormack, W. J. Chazin, T. E. Kehl-Fie and V. C. Culotta, *Infect. Immun.*, 2018, **86**, e00779–17.
- 35 T. G. Nakashige, J. R. Stephan, L. S. Cunden, M. B. Brophy, A. J. Wommack, B. C. Keegan, J. M. Shearer and E. M. Nolan, *J. Am. Chem. Soc.*, 2016, **138**, 12243–12251.
- 36 M. B. Brophy, T. G. Nakashige, A. Gaillard and E. M. Nolan, *J. Am. Chem. Soc.*, 2013, **135**, 17804–17817.
- 37 M. Brini, D. Ottolini, T. Cali and E. Carafoli, *Met. Ions Life Sci.*, 2013, **13**, 81–137.
- 38 J. Z. Liu, S. Jellbauer, A. J. Poe, V. Ton, M. Pesciaroli, T. E. Kehl-Fie, N. A. Restrepo, M. P. Hosking, R. A. Edwards, A. Battistoni, P. Pasquali, T. E. Lane, W. J. Chazin, T. Vogl, J. Roth, E. P. Skaar and M. Raffatellu, *Cell Host Microbe*, 2012, **11**, 227–239.
- 39 J. Wang, Z. R. Lonergan, G. Gonzalez-Gutierrez, B. L. Nairn, C. N. Maxwell, Y. Zhang, C. Andreini, J. A. Karty, W. J. Chazin, J. C. Trinidad, E. P. Skaar and D. P. Giedroc, *Cell Chem. Biol.*, 2019, **26**, 745–755.
- 40 E. M. Zygiel, C. E. Nelson, L. K. Brewer, A. G. Oglesby-Sherrouse and E. M. Nolan, *J. Biol. Chem.*, 2019, **294**, 3549–3562.
- 41 W. H. Lee, A. G. Oglesby and E. M. Nolan, *mSystems*, 2025, **10**, e0057625.
- 42 L. S. Cunden, M. B. Brophy, G. E. Rodriguez, H. A. Flaxman and E. M. Nolan, *Biochemistry*, 2017, **56**, 5726–5738.
- 43 C. A. Harrison, M. J. Raftery, J. Walsh, P. Alewood, S. E. Iismaa, S. Thliveris and C. L. Geczy, *J. Biol. Chem.*, 1999, **274**, 8561–8569.
- 44 I. S. M. Lee, M. Suzuki, N. Hayashi, J. Hu, L. J. van Eldik, K. Titani and M. Nishikimi, *Arch. Biochem. Biophys.*, 2000, **374**, 137–141.
- 45 B. Johne, M. K. Fagerhol, T. Lyberg, H. Prydz, P. Brandtzaeg, C. F. Naess-Andresen and I. Dale, *Mol. Pathol.*, 1997, **50**, 113–123.
- 46 D. Taylor and K. T. Holland, *J. Appl. Bacteriol.*, 1989, **66**, 319–329.
- 47 T. E. Kehl-Fie, Y. Zhang, J. L. Moore, A. J. Farrand, M. I. Hood, S. Rathi, W. J. Chazin, R. M. Caprioli and E. P. Skaar, *Infect. Immun.*, 2013, **81**, 3395–3405.
- 48 L. S. Cunden, A. Gaillard and E. M. Nolan, *Chem. Sci.*, 2016, **7**, 1338–1348.
- 49 J. N. Radin, J. L. Kelliher, P. K. P. Solórzano and T. E. Kehl-Fie, *PLoS Pathog.*, 2016, **12**, e1006040.
- 50 J. L. Harman, A. N. Loes, G. D. Warren, M. C. Heaphy, K. J. Lampi and M. J. Harms, *eLife*, 2020, **9**, e54100.
- 51 K. P. Grim, J. N. Radin, P. K. P. Solórzano, J. R. Morey, K. A. Frye, K. Ganio, S. L. Neville, C. A. McDevitt and T. E. Kehl-Fie, *J. Bacteriol.*, 2020, **202**, e00014–e00020.
- 52 A. Z. Velez, J. N. Radin, E. N. Kennedy, J. B. Parsons, H. M. Tong, E. Jung, E. Alam, L. C. Radlinski, N. J. Wagner, V. G. Fowler Jr, S. E. Rowe, T. Kehl-Fie and B. P. Conlon, *Proc. Natl. Acad. Sci. U. S. A.*, 2026, **123**, e2513462123.
- 53 A. Achouiti, T. Vogl, C. F. Urban, M. Röhm, T. J. Hommes, M. A. D. van Zoelen, S. Florquin, J. Roth, C. van't Veer, A. F. de Vos and T. van der Poll, *PLoS Pathog.*, 2012, **8**, e1002987.
- 54 M. I. Hood, B. L. Mortensen, J. L. Moore, Y. Zhang, T. E. Kehl-Fie, N. Sugitani, W. J. Chazin, R. M. Caprioli and E. P. Skaar, *PLoS Pathog.*, 2012, **8**, e1003068.
- 55 H. K. De Jong, A. Achouiti, G. C. K. W. Koh, C. M. Parry, S. Baker, M. A. Faiz, J. T. van Dissel, A. M. Vollaard, E. M. M. van Leeuwen, J. J. T. H. Roelofs, A. F. de Vos, J. Roth, T. van der Poll, T. Vogl and W. J. Wiersinga, *PLoS Neglected Trop. Dis.*, 2015, **9**, e0003663.
- 56 J. E. Cassat and E. P. Skaar, *Semin. Immunopathol.*, 2012, **34**, 215–235.
- 57 B. L. Mortensen and E. P. Skaar, *Front. Cell. Infect. Microbiol.*, 2013, **3**, 95.
- 58 G. Porcheron, A. Garenaux, J. Proulx, M. Sabri and C. M. Dozois, *Front. Cell. Infect. Microbiol.*, 2013, **3**, e00090.
- 59 L. D. Palmer and E. P. Skaar, *Annu. Rev. Genet.*, 2016, **50**, 67–91.



- 60 I. J. Schalk and O. Cunrath, *Environ. Microbiol.*, 2016, **18**, 3227–3246.
- 61 C. C. Murdoch and E. P. Skaar, *Nat. Rev. Microbiol.*, 2022, **20**, 657–670.
- 62 R. Garg, M. S. David, S. Yang and V. C. Culotta, *Annu. Rev. Microbiol.*, 2024, **78**, 23–38.
- 63 M. P. Mcnamara, C. Collins-Lech, J. H. Wiessner, B. L. Hahn and P. G. Sohnle, *Lancet*, 1988, **332**, 1163–1165.
- 64 A. R. Murthy, R. I. Lehrer, S. S. Harwig and K. T. Miyasaki, *J. Immunol.*, 1993, **151**, 6291–6301.
- 65 V. Santhanagopalan, B. L. Hahn and P. G. Sohnle, *J. Infect. Dis.*, 1995, **171**, 1289–1294.
- 66 P. G. Sohnle, B. L. Hahn and V. Santhanagopalan, *J. Infect. Dis.*, 1996, **174**, 1369–1372.
- 67 T. Okutomi, T. Tanaka, S. Yui, M. Mikami, M. Yamazaki, S. Abe and H. Yamaguchi, *Microbiol. Immunol.*, 1998, **42**, 789–793.
- 68 P. G. Sohnle, M. J. Hunter, B. Hahn and W. J. Chazin, *J. Infect. Dis.*, 2000, **182**, 1272–1275.
- 69 C. F. Urban, D. Ermert, M. Schmid, U. Abu-Abed, C. Goosmann, W. Nacken, V. Brinkmann, P. R. Jungblut and A. Zychlinsky, *PLoS Pathog.*, 2009, **5**, e1000639.
- 70 F. Citiulo, I. D. Jacobsen, P. Miramón, L. Schild, S. Brunke, P. Zipfel, M. Brock, B. Hube and D. Wilson, *PLoS Pathog.*, 2012, **8**, e1002777.
- 71 C. C. Staats, L. Kmetzsch, A. Schrank and M. H. Vainstein, *Front. Cell. Infect. Microbiol.*, 2013, **3**, 65.
- 72 B. Schwyn and J. B. Neilands, *Anal. Biochem.*, 1987, **160**, 47–56.
- 73 D. B. Alexander and D. A. Zuberer, *Biol. Fertil. Soils*, 1991, **12**, 39–45.
- 74 E. M. Zygiel, A. O. Obisesan, C. E. Nelson, A. G. Oglesby and E. M. Nolan, *J. Biol. Chem.*, 2021, **296**, 100160.
- 75 B. Korkmaz, M. S. Horwitz, D. E. Jenne and F. Gauthier, *Pharmacol. Rev.*, 2010, **62**, 726–759.
- 76 D. C. Whitcomb and M. E. Lowe, *Dig. Dis. Sci.*, 2007, **52**, 1–17.
- 77 P. H. Brown, A. Balbo and P. Schuck, *Curr. Protoc. Immunol.*, 2008, **81**, 1–39.
- 78 G. J. Howlett, A. P. Minton and G. Rivas, *Curr. Opin. Chem. Biol.*, 2006, **10**, 430–436.
- 79 W. H. Watson, J. Pohl, W. R. Montfort, O. Stuchlik, M. S. Reed, G. Powis and D. P. Jones, *J. Biol. Chem.*, 2003, **278**, 33408–33415.
- 80 H. J. Forman, H. Zhang and A. Rinna, *Mol. Aspects Med.*, 2009, **30**, 1–12.
- 81 R. Seitz, D. Tümen, C. Kunst, P. Heumann, S. Schmid, A. Kandulski, M. Müller and K. Gülow, *Antioxidants*, 2024, **13**, 1078.
- 82 A. Holmgren, *Annu. Rev. Biochem.*, 1985, **54**, 237–271.
- 83 J. E. Oblong and G. Powis, *FEBS Lett.*, 1993, **334**, 1–2.
- 84 T. Vogl, N. Leukert, K. Barczyk, K. Strupat and J. Roth, *Biochim. Biophys. Acta, Mol. Cell Res.*, 2006, **1763**, 1298–1306.
- 85 Y. R. Perera, K. T. Enriquez, A. Rodriguez, V. Garcia, T. Akizuki, A. Naretto, M. Togashi, R. Guillen, E. P. Skaar and W. J. Chazin, *Protein Sci.*, 2025, **34**, e70294.
- 86 K. Xie, M. Varatnitskaya, A. Maghnouj, V. Bader, K. F. Winklhofer, S. Hahn and L. I. Leichert, *Redox Biol.*, 2020, **28**, 101344.
- 87 F. G. Ottaviano, D. E. Handy and J. Loscalzo, *Circ. J.*, 2008, **72**, 1–16.
- 88 T. Vogl, K. Tenbrock, S. Ludwig, N. Leukert, C. Ehrhardt, M. A. D. van Zoelen, W. Nacken, D. Foell, T. van der Poll, C. Sorg and J. Roth, *Nat. Med.*, 2007, **13**, 1042–1049.
- 89 J. M. Ehrchen, C. Sunderkötter, D. Foell, T. Vogl and J. Roth, *J. Leukocyte Biol.*, 2009, **86**, 557–566.
- 90 M. Pruenster, A. R. M. Kurz, K.-J. Chung, X. Cao-Ehlker, S. Bieber, C. F. Nussbaum, S. Bierschenk, T. K. Eggersmann, I. Rohwedder, K. Heinig, R. Immler, M. Moser, U. Koedel, S. Gran, R. P. McEver, D. Vestweber, A. Verschoor, T. Leanderson, T. Chavakis, J. Roth, T. Vogl and M. Sperandio, *Nat. Commun.*, 2015, **6**, 6915.
- 91 T. Vogl, A. Stratis, V. Wixler, T. Völler, S. Thurainayagam, S. K. Jorch, S. Zenker, A. Dreiling, D. Chakraborty, M. Fröhling, P. Paruzel, C. Wehmeyer, S. Hermann, O. Papantonopoulou, C. Geyer, K. Loser, M. Schäfers, S. Ludwig, M. Stoll, T. Leanderson, J. L. Schultze, S. König, T. Pap and J. Roth, *J. Clin. Invest.*, 2018, **128**, 1852–1866.
- 92 S. F. Betz, *Protein Sci.*, 1993, **2**, 1551–1558.
- 93 M. Zavodszky, C. W. Chen, J. K. Huang, M. Zolkiewski, L. Wen and R. Krishnamoorthi, *Protein Sci.*, 2001, **10**, 149–160.
- 94 I. Cohen, M. Coban, A. Shahar, B. Sankaran, A. Hockla, S. Lacham, T. R. Caulfield, E. S. Radisky and N. Papo, *J. Biol. Chem.*, 2019, **294**, 5105–5120.
- 95 A. Zhou, R. W. Carrell, M. P. Murphy, Z. Wei, Y. Yan, P. L. D. Stanley, P. E. Stein, F. B. Pipkin and R. J. Read, *Nature*, 2010, **468**, 108–111.
- 96 M. Steglich, R. Lombide, I. López, M. Portela, M. Fló, M. Marín, B. Alvarez and L. Turell, *PLoS One*, 2020, **15**, e0240580.
- 97 A. Kawakami, K. Kubota, N. Yamada, U. Tagami, K. Takehana, I. Sonaka, E. Suzuki and K. Hirayama, *FEBS J.*, 2006, **273**, 3346–3357.
- 98 Y. Iwao, M. Anraku, M. Hiraike, K. Kawai, K. Nakajou, T. Kai, A. Suenaga and M. Otagiri, *Drug Metab. Pharmacokinet.*, 2006, **21**, 140–146.
- 99 R. Deshpande, T. L. Woods, J. Fu, T. Zhang, S. W. Stoll and J. T. Elder, *J. Invest. Dermatol.*, 2000, **115**, 477–485.
- 100 T. Zhang, T. L. Woods and J. T. Elder, *J. Invest. Dermatol.*, 2002, **119**, 1196–1201.
- 101 M. Koch, J. Diez and G. Fritz, *Acta Crystallogr., Sect. F: Struct. Biol. Cryst. Commun.*, 2006, **62**, 1120–1123.
- 102 C. Haase-Kohn, S. Wolf, J. Lenk and J. Pietzsch, *Biochem. Biophys. Res. Commun.*, 2011, **413**, 494–498.
- 103 M. Tsuchiya, F. Yamaguchi, S. Shimamoto, T. Fujimoto, H. Tokumitsu, M. Tokuda and R. Kobayashi, *Int. J. Mol. Med.*, 2014, **34**, 1713–1719.
- 104 S. Réty, D. Osterloh, J.-P. Arié, S. Tabaries, J. Seeman, F. Russo-Marie, V. Gerke and A. Lewit-Bentley, *Structure*, 2000, **8**, 175–184.



- 105 S. Saho, H. Satoh, E. Kondo, Y. Inoue, A. Yamauchi, H. Murata, R. Kinoshita, K.-I. Yamamoto, J. Futami, E. W. Putranto, I. M. W. Ruma, I. W. Sumardika, C. Youyi, K. Suzawa, H. Yamamoto, J. Soh, S. Tomida, Y. Sakaguchi, K. Saito, H. Iioka, N.-H. Huh, S. Toyooka and M. Sakaguchi, *Cancer Microenviron.*, 2016, **9**, 93–105.
- 106 K. Z. Hein, H. Takahashi, T. Tsumori, Y. Yasui, Y. Nanjoh, T. Toga, Z. Wu, J. Grötzinger, S. Jung, J. Wehkamp, B. O. Schroeder, J. M. Schroeder and E. Morita, *Proc. Natl. Acad. Sci. U. S. A.*, 2015, **112**, 13039–13044.
- 107 J. S. Cristóvão, G. G. Moreira, F. E. P. Rodrigues, A. P. Carapeto, M. S. Rodrigues, I. Cardoso, A. E. N. Ferreira, M. Machuqueiro, G. Fritz and C. M. Gomes, *Chem. Commun.*, 2021, **57**, 379–382.
- 108 S. Y. Lim, M. J. Raftery, J. Goyette, K. Hsu and C. L. Geczy, *J. Leukocyte Biol.*, 2009, **86**, 577–587.
- 109 L. Signor, T. Paris, C. Mas, A. Picard, G. Lutfalla, E. B. Erba and L. Yatime, *J. Struct. Biol.*, 2021, **213**, 107689.
- 110 A. Mueller, B. W. Schäfer, S. Ferrari, M. Weibel, M. Makek, M. Höchli and C. W. Heizmann, *J. Biol. Chem.*, 2005, **280**, 29186–29193.
- 111 A. S. DiChiara, R. C. Li, P. H. Suen, A. S. Hosseini, R. J. Taylor, A. F. Weickhardt, D. Malhotra, D. R. McCaslin and M. D. Shoulders, *Nat. Commun.*, 2018, **9**, 4206.
- 112 D. M. Pinkas, P. Strop, A. T. Brunger and C. Khosla, *PLoS Biol.*, 2007, **5**, e327.
- 113 A. V. Melkonian, E. Loppinet, R. Martin, M. Porteus and C. Khosla, *J. Am. Chem. Soc.*, 2021, **143**, 10537–10540.
- 114 A. S. Sewa, H. A. Besser, I. I. Mathews and C. Khosla, *Proc. Natl. Acad. Sci. U. S. A.*, 2024, **121**, e2407066121.

